Efficient Circuit-Level Analysis of Large Microwave Systems by Krylov-Subspace Harmonic Balance

Vittorio Rizzoli (1), Alessandro Lipparini (1), Diego Masotti (1), and Franco Mastri (2)

(1) DEIS, University of Bologna, Villa Griffone, 40044 Pontecchio Marconi (BO), Italy
(2) DIE, University of Bologna, Viale Risorgimento 2, 40136 Bologna, Italy

Abstract — **The paper proposes a rigorous harmonic-balance technique for the circuit-level simulation of complex microwave systems consisting of many interconnected functional blocks. The voltages at the interface ports between building blocks are used as auxiliary unknowns, and are determined simultaneously with the block state variables by a Krylov-subspace inexact Newton iteration. This provides exact results and allows large savings of both memory and CPU time.**

I. INTRODUCTION

The circuit-level simulation of complex microwave systems by rigorous harmonic-balance (HB) methods is a computationally intensive task even if efficient Krylov-subspace techniques are adopted in the solution process. Indeed, if realistic topologies are considered, even a conventional quasi-periodic analysis under multitone excitation may require several million nodal unknowns, and thus days of CPU time, and physical memory in the gigabyte range. If the system consists of several interconnected functional blocks, a possible way out is to perform the simulation with the aid of behavioral models of the individual subsystems. These models are computationally fast, but always rely upon some kind of approximation, such as the assumptions of narrow-band signal spectra or unilateral signal flow, that may result in significant losses of accuracy. The tradeoff can be improved either by resorting to more sophisticated behavioral models [1], [2], or by enhancing the efficiency of system-oriented HB simulation. In this paper we present a method of the second kind, that can optimally exploit the block structure of the system to be analysed. The basic idea is to introduce a set of auxiliary state variables (SV) consisting of the voltages at the subsystem ports, which creates in the Jacobian matrix a well-defined sparsity pattern. Such sparsity can be effectively exploited in a hierarchical solution approach if ordinary HB techniques are used [3], or in the simultaneous solution for all the unknowns when the HB analysis is performed by Krylov-subspace methods [4], as we propose in this paper. We show that the overhead introduced by the auxiliary unknowns is normally small, so that important savings of both memory and CPU time are obtained, and really huge simulation tasks may be brought within the reach of ordinary workstations or even PC's. All the nonlinear interactions between subsystems are exactly accounted for in the analysis, both in band and out of band, and all the peculiar advantages of SV-based HB analysis [5], [6] are fully retained by the new technique. In particular, an arbitrary number of linear subsystems of any complexity may be included in the system without substantially affecting memory and CPU time requirements.

II. EFFICIENT CIRCUIT-LEVEL SYSTEM ANALYSIS

Let us consider a microwave system resulting from the interconnection of B nonlinear subsystems (blocks) which only interact through the connecting ports. The b-th block ($1 \le b \le B$) is subdivided into a linear and a nonlinear subnetwork interconnected through N_b device ports. The linear subnetwork has a total of E_b external ports, M_b of which are used for connection with other blocks, while the remaining ones are connected with sources or loads. The number of inter-block connecting ports is arbitrary, but will be assumed to be small with respect to the total number of device ports. Voltages and currents at the b-th block device ports will be stacked in two N_b-vectors $\mathbf{v_D}^{(b)}(t)$, $\mathbf{i_D}^{(b)}(t)$. The currents at the device ports are considered positive when entering the nonlinear subnetwork. Under the assumption of multitone excitation of the system, the generic (**k**-th) intermodulation (IM) product of the exciting fundamental frequencies will be denoted by $\Omega_\mathbf{k}$ where **k** is a vector of harmonic numbers. The N_b-vectors containing the **k**-th voltage and current harmonics at the device ports will be denoted by $\mathbf{V_{Dk}}^{(b)}$, $\mathbf{I_{Dk}}^{(b)}$. Similarly, the **k**-th (scalar) harmonics of the voltage and current at the h-th external connection port of the b-th block linear subnetwork ($1 \le h \le M_b$) will be denoted by $V_{h\mathbf{k}}^{(b)}$, $I_{h\mathbf{k}}^{(b)}$. The currents at the external ports are considered positive when entering the linear subnetwork.

After connecting the exciting sources to the respective blocks, the b-th block linear subnetwork may be described in terms of a $(N_b + M_b) \times (N_b + M_b)$ admittance matrix and a $(N_b + M_b)$ vector of equivalent Norton current sources. The admittance matrix at the generic IM product Ω_k will be denoted by

$$\mathbf{Y}^{(b)}(\Omega_k) = \left[\begin{array}{c|c} \mathbf{Y_{DD}}^{(b)}(\Omega_k) & \mathbf{Y_{DE}}^{(b)}(\Omega_k) \\ \hline \mathbf{Y_{ED}}^{(b)}(\Omega_k) & \mathbf{Y_{EE}}^{(b)}(\Omega_k) \end{array}\right] \quad (1)$$

where the subscripts "D", "E" stand for "device ports" and "external ports", respectively. The linear subnetwork equations for the b-th block at Ω_k then take on the form

$$-\mathbf{I_{Dk}}^{(b)} = \mathbf{Y_{DD}}^{(b)}(\Omega_k)\, \mathbf{V_{Dk}}^{(b)} + \mathbf{N_D}^{(b)}(\Omega_k) + \sum_{m=1}^{M_b} \mathbf{Y_{DEm}}^{(b)}(\Omega_k)\, V_{mk}^{(b)}$$

$$I_{hk}^{(b)} = \mathbf{Y_{EDh}}^{(b)}(\Omega_k)\, \mathbf{V_{Dk}}^{(b)} + N_h^{(b)}(\Omega_k) + \sum_{m=1}^{M_b} Y_{EEhm}^{(b)}(\Omega_k)\, V_{mk}^{(b)} \quad (2)$$

$(1 \le h \le M_b)$

where the $\mathbf{N}$'s are vectors of equivalent Norton current sources at the ports, and the admittance symbols have the following meanings:

$\mathbf{Y_{DEm}}^{(b)}(\Omega_k)$ = m-th column of $\mathbf{Y_{DE}}^{(b)}(\Omega_k)$

$\mathbf{Y_{EDh}}^{(b)}(\Omega_k)$ = h-th row of $\mathbf{Y_{ED}}^{(b)}(\Omega_k)$ (3)

$Y_{EEhm}^{(b)}(\Omega_k)$ = scalar entry of $\mathbf{Y_{EE}}^{(b)}(\Omega_k)$ belonging to the h-th row and to the m-th column

The nonlinear subnetwork (device) equations for the b-th block will be cast in the parametric form [5]

$$\mathbf{v_D}^{(b)}(t) = \mathbf{u}^{(b)}\left[\mathbf{x}^{(b)}(t), \frac{d\mathbf{x}^{(b)}(t)}{dt}, \ldots, \mathbf{x_d}^{(b)}(t)\right]$$

$$\mathbf{i_D}^{(b)}(t) = \mathbf{w}^{(b)}\left[\mathbf{x}^{(b)}(t), \frac{d\mathbf{x}^{(b)}(t)}{dt}, \ldots, \mathbf{x_d}^{(b)}(t)\right] \quad (4)$$

where $\mathbf{x}^{(b)}$ is an N_b-vector of SV pertaining to the block, and $\mathbf{x_d}^{(b)}$ is an N_b-vector of time-delayed SV [5]. Let us now introduce a state vector $\mathbf{X}^{(b)}$ containing the real and imaginary parts of all SV harmonics for the b-th block. The voltages at the external connection ports of the blocks are assigned the role of auxiliary SV, so that the vectors $\mathbf{X}^{(b)}$ and the harmonics $V_{mk}^{(b)}$ $(1 \le m \le M_b)$ of the auxiliary SV represent the problem unknowns $(1 \le b \le B)$.

At the device ports of the b-th subsystem the following equations must be satisfied:

$$\mathbf{U_k}^{(b)}\left[\mathbf{X}^{(b)}\right] = \mathbf{V_{Dk}}^{(b)}$$

$$\mathbf{W_k}^{(b)}\left[\mathbf{X}^{(b)}\right] = \mathbf{I_{Dk}}^{(b)} \quad (5)$$

where $\mathbf{U_k}^{(b)}$, $\mathbf{W_k}^{(b)}$ are the $\mathbf{k}$-th harmonics of (4). By replacing (5) into the first of (2), the b-th subsystem HB equations at Ω_k may be written in the form

$$\mathbf{Y_{DD}}^{(b)}(\Omega_k)\, \mathbf{U_k}^{(b)}\left[\mathbf{X}^{(b)}\right] + \mathbf{W_k}^{(b)}\left[\mathbf{X}^{(b)}\right] + \mathbf{N_D}^{(b)}(\Omega_k) + \sum_{m=1}^{M_b} \mathbf{Y_{DEm}}^{(b)}(\Omega_k)\, V_{mk}^{(b)} = \mathbf{0} \quad (6)$$

Note that the first row of (6) represents the vector of complex HB errors that should be equated to zero in order to perform a separate HB analysis of the b-th block (with the connecting ports short-circuited). In order to complete the set of system equations, (6) must be complemented by the connection equations. As an example, if the h-th port of the p-th block is connected with the r-th port of the q-th block, the corresponding connection equations become

$$\begin{cases} V_{hk}^{(p)} - V_{rk}^{(q)} = 0 \\ I_{hk}^{(p)} + I_{rk}^{(q)} = 0 \end{cases} \quad \forall \mathbf{k} \quad (7)$$

The total number of connection equations (7) will be denoted by $2N_C$. Combining the second of (2) with the second of (7) generates an additional set of HB equations of the form

$$\mathbf{Y_{EDh}}^{(p)}(\Omega_k)\, \mathbf{U_k}^{(p)}\left[\mathbf{X}^{(p)}\right] + \mathbf{Y_{EDr}}^{(q)}(\Omega_k)\, \mathbf{U_k}^{(q)}\left[\mathbf{X}^{(q)}\right] + \sum_{m=1}^{M_p} Y_{EEhm}^{(p)}(\Omega_k)\, V_{mk}^{(p)} + \sum_{j=1}^{M_q} Y_{EErj}^{(q)}(\Omega_k)\, V_{jk}^{(q)} + N_h^{(p)}(\Omega_k) + N_r^{(q)}(\Omega_k) = 0 \quad (8)$$

The nonlinear solving system is the set of equations (6), (8), for $1 \le b \le B$ and for all combinations of h, p, r, q appearing in (7). The Jacobian matrix of such system may be partitioned as follows:

$$\mathbf{J} = \left[\begin{array}{c|c} \mathbf{J_{BB}} & \mathbf{J_{BC}} \\ \hline \mathbf{J_{CB}} & \mathbf{J_{CC}} \end{array}\right] \qquad (9)$$

where the subscripts "B", "C", are associated with the HB equations and the SV harmonics pertaining to the nonlinear blocks and to the inter-block connections, respectively. The strucure of the Jacobian submatrices will now be examined in some detail. Due to (6), $\mathbf{J_{BB}}$ is block-diagonal, and may be written in the form

$$\mathbf{J_{BB}} = \mathrm{diag}\left[\mathbf{J}^{(1)}, \mathbf{J}^{(2)}, \mathbf{J}^{(3)}, \ldots\ldots, \mathbf{J}^{(B)}\right] \qquad (10)$$

where $\mathbf{J}^{(b)}$ $(1 \le b \le B)$ is the (dense) Jacobian matrix of the ordinary HB system for the b-th block, when such block is separately analysed with all connection ports short-circuited. $\mathbf{J_{BC}}$ is generated by the linear part (second row) of the HB equations (6), so that its submatrices are real and imaginary parts of the column vectors $\mathbf{Y_{DEm}}^{(b)}(\Omega_k)$. $\mathbf{J_{BC}}$ is thus sparse, with only $2M_b$ nonzero elements per row. $\mathbf{J_{CB}}$ and $\mathbf{J_{CC}}$ are generated by the connection equations (7). The N_C rows of $\mathbf{J_{CB}}$ originating from the first of (7) are obviously zero, while the corresponding rows of $\mathbf{J_{CC}}$ have only two nonzero entries equal to ± 1. The remaining part of $\mathbf{J_{CB}}$ is generated by the nonlinear part (i.e., the first row) of (8), and may thus be partitioned into submatrices of the general form

$$\mathrm{Re}\left[\mathbf{Y_{EDm}}^{(b)}(\Omega_k)\right] \frac{\partial F\left[\mathbf{U_k}^{(b)}\right]}{\partial F\left[\mathbf{X_s}^{(b)}\right]} \pm \pm \mathrm{Im}\left[\mathbf{Y_{EDm}}^{(b)}(\Omega_k)\right] \frac{\partial F\left[\mathbf{U_k}^{(b)}\right]}{\partial F\left[\mathbf{X_s}^{(b)}\right]} \qquad (11)$$

where $\mathbf{X_s}^{(b)}$ is the vector of the s-th harmonics of $\mathbf{x}^{(b)}(t)$, and the operator $F[\bullet]$ may denote either the real or the imaginary part, in any combination. A row of this section of $\mathbf{J_{CB}}$ associated with the p-th and q-th blocks has $(N_p + N_q)(2P + 1)$ nonzero entries, where P is the number of positive IM products taken into account in the HB analysis. Finally, the remaining N_C rows of $\mathbf{J_{CC}}$ are generated by the linear part (i.e., the second row) of (8), so that their entries are real and imaginary parts of the admittance parameters $Y_{EEmn}{}^{(b)}(\Omega_k)$. $\mathbf{J_{CC}}$ is also sparse, with only $2(M_p + M_q)$ nonzero elements per row.

Let us now assume that the nonlinear system is solved by a Krylov-subspace technique. With this class of methods, the bulk of the CPU time is spent in the multiplication of the Jacobian matrix by a sequence of real vectors [4]. It is thus obvious that the structure (9) of the Jacobian matrix with the above discussed properties is particularly well suited for this solution approach, because the multiplication process can take full advantage of the fixed sparsity pattern of the Jacobian sub-matrices. In particular, if the number of auxiliary SV is relatively small (say, 10% of the total or less), which is often the case in practice, the dominant contribution to the multiplication time is due to $\mathbf{J_{BB}}$, and the overhead due to the remaining submatrices is small.

III. A Performance Benchmark

Let us consider a typical single-conversion receiver front-end, whose functional diagram in terms of interconnected blocks is given in fig. 1. The circuit basically consists of two doubly balanced mixers arranged in an image-rejection configuration, a local oscillator, coupling networks, amplifiers, and filters. The band of operation is 935 - 960 MHz and the IF is 90 MHz. The circuit-level description of the front-end is very detailed, and includes many (linear) parasitic components. The total number of device ports is $n_D = 208$, and the total number of nodes is 1745. A two-tone IM analysis of the front-end is carried out with 0 dBm of LO power and an RF excitation consisting of two tones of equal amplitudes. The RF power is swept from -50 to 0 dBm per tone (the latter corresponding to a gain compression of about 36 dB). Such high signal levels are considered in order to give a clear account of the excellent power handling capabilities of the analysis algorithm. 6 LO harmonics and IM products of the two RF signals up to the 7th order are taken into account in the analysis, for a total of 734 positive frequencies and 2,563,405 nodal unknowns. If the system is treated as a whole, the CPU time is about 19,600 seconds per power point, and the memory occupation is about 1,870 MB on a SUN Enterprise 450 workstation. The front-end is then subdivided into 9 interconnected blocks (5 three-ports and 4 two-ports) in the way shown in fig. 1, which requires the introduction of 20 auxiliary SV. With the algorithm discussed in this paper, the CPU time for the same analysis is reduced to about 4,800 seconds per power point, and the total memory occupation to about 620 MB on the same workstation. The numerical results are shown in fig. 2, and are strictly identical in both cases.

The speed and memory advantage quickly increase with the number of nonlinear devices contained in the system.

References

[1] J. S. Kenney and A. C. Cova, "Advances in behavioral modeling techniques for microwave circuits and subsystems", *Digest of IEEE MTT-S Workshop WSJ: New Developments in Mixed-Mode Techniques for Nonlinear Circuit Design*, Boston, MA, June 2000, pp. 112-151.

[2] Y. Harkouss *et al.*, "The use of artificial neural networks in nonlinear microwave devices and circuits modeling: an application to telecommunication system design", *Int. Journal RF and Microwave Computer-Aided Eng.*, vol. 9, May 1999, pp. 198-215.

[3] V. Rizzoli, F. Mastri, and D. Masotti, "A hierarchical harmonic-balance technique for the efficient simulation of large-size nonlinear microwave circuits", *Proc. 25th European Microwave Conference*, Sept. 1995, pp. 615-619.

[4] V. Rizzoli *et al.*, "Fast and robust inexact-Newton approach to the harmonic-balance analysis of nonlinear microwave circuits", *IEEE Microwave Guided Waves Lett.*, Vol. 7, Oct. 1997, pp. 359-361.

[5] V. Rizzoli *et al.*, "State-of-the-art harmonic-balance simulation of forced nonlinear microwave circuits by the piecewise technique", *IEEE Trans. Microwave Theory Tech.*, Vol. 40, Jan. 1992, pp. 12-28.

[6] M. B. Steer *et al.*, "Global modeling of spatially distributed Microwave and millimeter-wave systems", *IEEE Trans. Microwave Theory Tech.*, Vol. 47, June 1999, pp. 830-839.

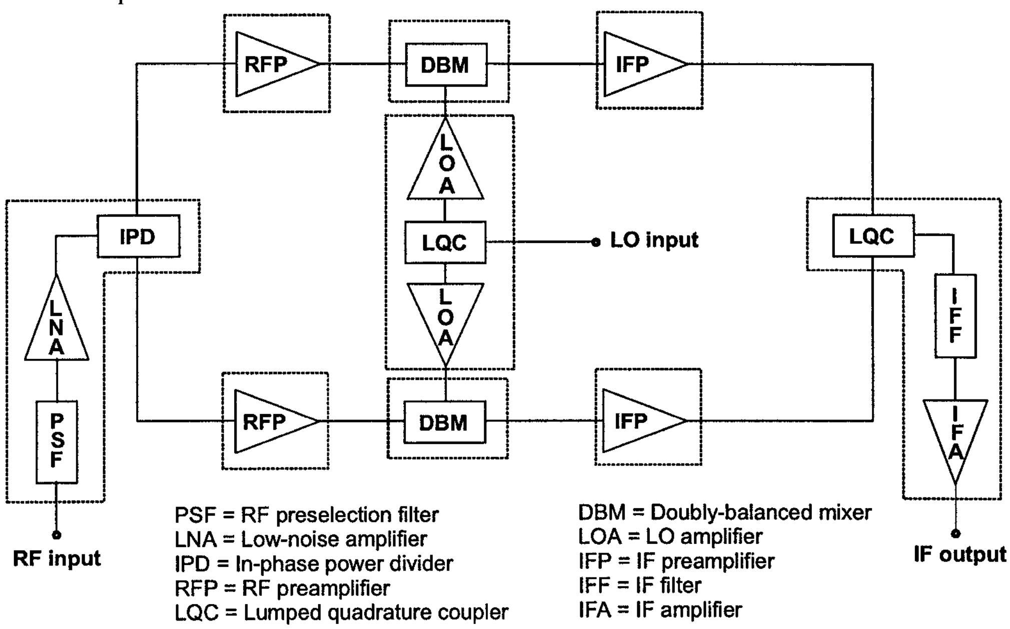

Fig. 1. Schematic topology of a microwave front-end

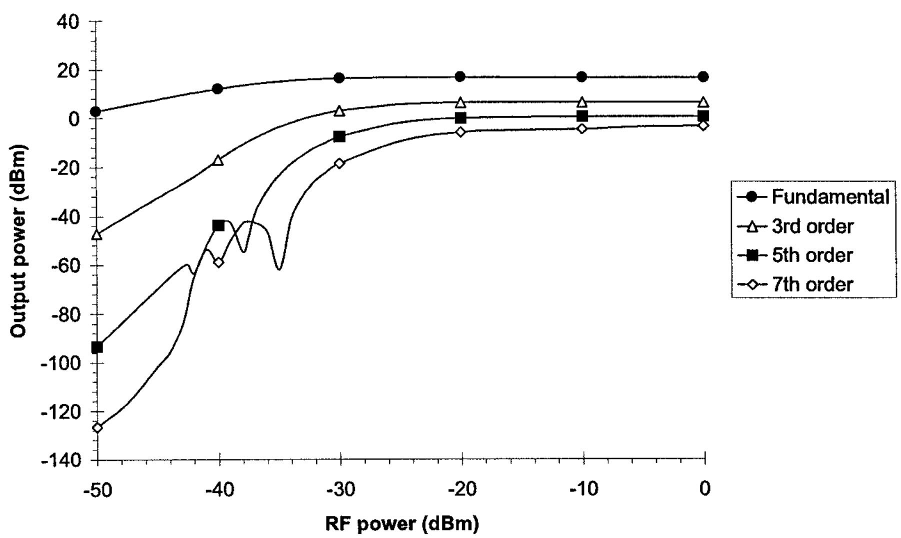

Fig. 2. Spectral components at the front-end output